Structural and Functional Characteristics of Chimeric Avidins Physically Adsorbed onto Functionalized Polythiophene Thin Films

ARTICLE *in* ACS APPLIED MATERIALS & INTERFACES · JULY 2012

Impact Factor: 6.72 · DOI: 10.1021/am3008517 · Source: PubMed

8 AUTHORS, INCLUDING:

Jani Pelto
VTT Technical Research Centre of Finland
21 PUBLICATIONS **143** CITATIONS
SEE PROFILE

Juha A E Määttä
University of Tampere
33 PUBLICATIONS **367** CITATIONS
SEE PROFILE

Abderrahim Yassar
École Polytechnique
132 PUBLICATIONS **5,815** CITATIONS
SEE PROFILE

Inger Vikholm-Lundin
University of Tampere
77 PUBLICATIONS **996** CITATIONS
SEE PROFILE

ACS APPLIED MATERIALS & INTERFACES

Research Article

www.acsami.org

Structural and Functional Characteristics of Chimeric Avidins Physically Adsorbed onto Functionalized Polythiophene Thin Films

Willem M. Albers,*[,†] Jani M. Pelto,[†] Clément Suspène,[‡] Juha A. Määttä,[§] Abderrahim Yassar,[⊥] Vesa P. Hytönen,[§,#] Inger M. Vikholm-Lundin,[†] and Kirsi Tappura[†]

[†]VTT Technical Research Centre of Finland, Sinitaival 6 FI-33720 Tampere, Finland

[‡]Laboratoire Itodys - UMR 7086, Université Paris Diderot, Université Paris 7 Diderot - Bâtiment Lavoisier, 15 rue Jean-Antoine de Baïf, 75205 Paris, France.

[§]IBT Institute of Biomedical Technology, University of Tampere, BioMediTech and Tampere University Hospital, Biokatu 6, 33014 University of Tampere, Finland

[⊥]LPICM, UMR 7647 CNRS, Ecole polytechnique, route de Saclay, 91128, Palaiseau Cedex, France.

[#]Centre for Laboratory Medicine, Tampere University Hospital, 33520 Tampere, Finland

Supporting Information

ABSTRACT: Stabilized bioreceptor layers are of great importance in the design of novel biosensors. In earlier work, chimeric avidins enabled immobilization of biotinylated antibodies onto gold surfaces with greater stability compared to more conventional avidins (wild-type avidin and streptavidin). In the present study, the applicability of chimeric avidins as a general binding scaffold for biotinylated antibodies on spin-coated functionalized polythiophene thin films has been studied by surface plasmon resonance and atomic force microscopy. Novel chimeric avidins showed remarkably increased binding characteristics compared with other avidins, such as wild-type avidin, streptavidin, and bacterial avidin when merely physically adsorbed onto the polythiophene surface. They gave the highest binding capacities, the highest affinity constant, and the highest stability for biotinylated probe immobilization. Introduction of carboxylic acid groups to polythiophene layer further enhanced the binding level of the avidins. Polythiophene layers functionalized with chimeric avidins thus offered a promising generic platform for biosensor applications.

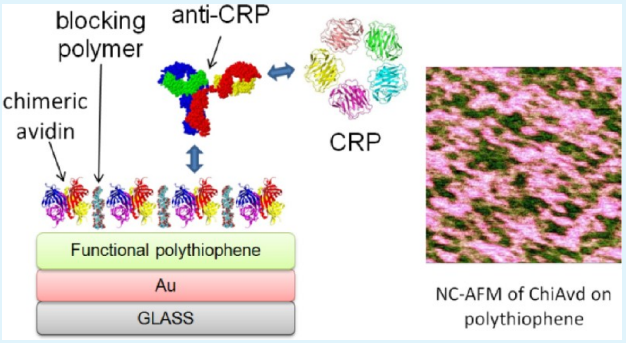

KEYWORDS: *chimeric avidin, polythiophene, C-reactive protein, antibody immobilization, surface plasmon resonance, atomic force microscopy*

1. INTRODUCTION

Biomolecules generally show quite strong, irreversible adsorption to hydrophobic surfaces. In many cases, strong conformational changes take place, in which the hydrophobic inner domain of the protein becomes exposed to the surface and significant spreading occurs, leading to loss of functionality/activity. For instance, with polystyrene surfaces only up to about 3−10% of the binding sites of IgG antibodies remain active.[1,2] However, hydrophobic polymer substrates can still be of practical use, as the sensitivity of an assay based on immunoreactions is proportional to the product of the affinity constant (K_A) and binding capacity (Γ).

One particularly interesting hydrophobic polymer is poly(3-hexylthiophene), P3HT, which is used in organic field-effect transistor (OFET) applications.[4,5] However, with respect to deposition of bioreceptor layers onto native P3HT, no detailed reports have yet appeared, although a preliminary study was conducted for poly(3,4-ethylenedioxythiophene) (PEDOT), in which the binding of rabbit IgG to goat antirabbit IgG was investigated.[7] Recently, also imprinted layers of avidin were reported in PEDOT/PSS matrices with selective binding to avidin, as studied with fluorescence, surface plasmon resonance (SPR), and quartz crystal microbalance (QCM) techniques. However, binding of biotin or biotinylated biomolecules to the avidin was not studied.[8] Optimization of the activity of biotinylated probes on P3HT surfaces is the first step on the way to a functional OFET device, and this can be favorably studied with QCM or SPR techniques, which directly measure the surface coverage, in contrast to the OFET, of which the charge displacement is measured at the interface of the organic layer of the FET device.[9]

As a highly hydrophobic material, the application of P3HT suffers from the drawback that the introduction of functional groups and further covalent linkage to bulky biomolecules will

Received: May 14, 2012
Accepted: July 12, 2012
Published: July 12, 2012

Scheme 1. Structures of the Compounds Used in This Study

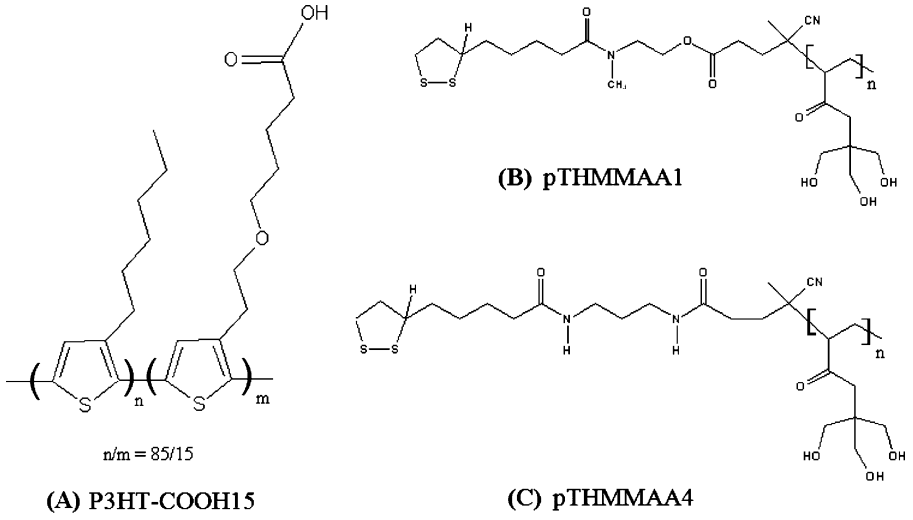

easily disturb the planar conformation and packing of the thiophene groups in the interfacial region, needed for optimal OFET characteristics.[10] Thus, for the development and commercial implementation of any OFET-based biosensors, direct adsorption of biomolecules onto P3HT is the first method to be considered for facile mass fabrication. Additionally, the use of a generic binding scaffold, such as avidin is also very much favored. Although it requires the use of more expensive biotinylated receptors, it would provide a more broadly applicable immobilization strategy. The use of generic binder reduces significantly the need for optimization of conditions in the biofunctionalization. Furthermore, biotinylated reagents are already widely available, and biotinylation does not require special equipment. Recently, chimeric avidins have been produced with greatly increased conformational stability, which yielded good resistance against heating, organic solvents, and drying,[11] and bioactive inks have been produced of chimeric avidins for printable diagnostic applications.[12]

The present study focuses on the adsorption of various avidins (two wild-type avidins, streptavidin, and two chimeric avidins) on three types of polythiophene surfaces, relevant to the construction of a FET-based biosensor. The polymers were spin-coated onto gold substrates, and surface plasmon resonance (SPR) and atomic force microscopy were used to characterize the polythiophene layer and the formed avidin layers. The binding characteristics of biotinylated antibodies to the avidins were studied for each type of surface, as well as the binding of the antigen to the biotinylated probes. Two biotinylated antibody preparations were used, one specific for human IgG and the other for C-reactive protein (CRP). Various aspects of the optimization of the binding were investigated, such as the kinetic adsorption behavior of the different avidins to three types of polythiophene layers, assessment and optimization of the activity of biotinylated antibodies, using Tween 20 and two tris-hydroxymethylmethyl acrylamide polymers, which were previously tested on gold surfaces, for lowering nonspecific binding.[13,14] Furthermore, preliminary tests were performed to assess the effect of printing methods for the avidins and the biotinylated antibodies. Also preliminary AFM images were acquired to uncover the differences in surface structural features of the avidin films on P3HT.

2. EXPERIMENTAL SECTION

2.1. Chemicals and Substrates. The solvents, chloroform, and DMF (from J. T. Baker or Merck) were all of analytical grade. Milli-Q water with a resistance larger than 18 MΩ and a TOC lower than 4 ppb was used in all experiments. Gold substrates for SPR were prepared by RF magnetron sputtering, using an Edwards E306A two-target sputter coater, employing an intermediate layer of ITO as described in detail elsewhere.[17] Electronic grade poly[3-hexylthiophene] (P3HT) and poly[3-(5-carboxypentyl)-thiophene] (P3CPT) both with 90−93% regioregularity where obtained from Rieke Metals Inc. P3HT-COOH15 with carboxylic acid terminated side chains (Scheme 1A) was prepared according to previously reported methods.[18,19]

Phosphate buffered saline solution (PBS) consisted of 150 mM NaCl and 10 mM sodium phosphate, pH 7.45. Tween 20 (Biograde) and bovine serum albumin (BSA, 98% purity by electrophoresis) were obtained from Sigma-Aldrich. The blocking polymers pTHMMAA1 and pTHMMAA4 (Scheme 1B,C) were produced as freeze-dried preparation, as reported previously.[13−16] The polymers were reconstituted in PBS at a concentration of 1 mg/mL.

Wild type avidin (wt-Avd, MW ≈ 63 kDa, pI = 9.7) from chicken egg white was obtained from Belovo SA. Chimeric avidin, (ChiAvd, MW = 57.5 kDa, pI = 9.7[20]), cysteine-tagged chimeric avidin (ChiAvd-Cys, MW = 57.9 kDa, pI = 9.6[12]), and bacterially expressed chicken avidin (b-Avd, MW = 8.7 kDa, pI = 9.7[21]) were produced in BL21-AI *E. coli* cells (Invitrogen) by fed-batch fermentation and purified with affinity chromatography using 2-iminobiotin-Sepharose 4 Fast Flow (Affiland S.A. Liege, Belgium, prod. no. IMI-H-4FF) as described earlier.[22] Streptavidin (SA) was obtained from Jackson ImmunoResearch (Prod. No. 016−000−084, MW=55 kD) as a freeze-dried powder and after reconstitution with Milli-Q water yielded a stock solution containing 2 mg/mL streptavidin and 0.2 mg/mL NaCl. Biotinylated goat antihuman IgG, a biotin-SP-conjugate of the $F(ab')_2$-fragment, was obtained from Jackson ImmunoResearch (Prod. No. 109−066−098). The freeze-dried powder was reconstituted with Milli-Q water to a concentration of 1.5 mg/mL, yielding a buffer containing 10 mM sodium phosphate, pH = 7.6, 250 mM NaCl, 15 mg/mL BSA and 0.05% sodium azide. For comparison, the nonbiotinylated $F(ab')_2$-fragment and whole IgG antibody, both affinity-purified, were obtained from the same manufacturer (Prod. No. 109−006−098 and 109−005−098 respectively). Biotinylated anti-CRP was obtained from HyTest OY (Turku, Finland) as a stock solution of 0.9 mg/mL in a buffer containing 20 mM TRIS-HCl, pH = 7.5, 250 mM NaCl and 0.1% sodium azide. Chromatographically purified human IgG (h-IgG) was obtained from Jackson ImmunoResearch (Prod. No. 009−000−003) at a concentration of 11 mg/mL. Plasma CRP was purchased from Scripps laboratories (San Diego, CA, USA) at a stock

concentration 2.6 mg/mL in 20 mM TRIS-HCl, 280 mM NaCl, 5 mM $CaCl_2$, and 0.1% sodium azide.

2.2. Deposition of Polymers onto Gold. P3HT and P3HT-COOH15 were spin-coated onto the gold using a concentration of 1.25 or 2.5 mg/mL in chloroform, while P3CPT was spin-coated from DMF at 2.5 mg/mL. Spin-coating was conducted on a Laurel WS 400 spin coater for 30 s at 2000 rpm. To obtain optimal film uniformity and low surface roughness without particulates, the solution was passed through a cellulose filter in the form of a small piece of laboratory tissue propped tightly into a Pasteur pipet. The surface was fully covered with the solution for 5−10 s to allow proper wetting before spinning. Thickness of the polymer film was determined with SPR spectroscopy and AFM imaging.

2.3. SPR MEASUREMENTS

SPR measurements were performed either on a Biacore 3000 instrument (GE Healthcare/Biacore AB, Uppsala, Sweden), or an SPR-Navi 200 angle-scanning SPR instrument (BioNavis Ltd., Tampere, Finland). The former instrument was used for kinetic measurements and evaluation of antigen binding characteristics, while the angle-scanning instrument was used for assessment of the thickness and refractive index of the polythiophene layers, using measurements in two optical media.[23] With the Biacore instrument the approximation that 1 resonance unit (RU) corresponds to 1 pg/mm^2 of adsorbed protein was used throughout.[24] However, this approximation does not hold for the polythiophene layers, of which the refractive index is much higher than that of proteins: (1.6−1.7 for P3HT compared to 1.42−1.45 for proteins).[25]

2.4. Avidin and Antibody Immobilization. In immobilization experiments the P3HT substrates of size 9 × 12 mm were glued with double-sticking tape in a plastic frame of a Biacore 3000 chip cassette. Avidins were immobilized by flow injection in the Biacore 3000 instrument, after docking the chip and performing a single prime operation to stabilize the surface in PBS, which comprises washing of the syringes and microfluidic cartridge with fresh PBS buffer. Before docking a new chip, always a desorb routine and a prime routine were run with a maintenance chip docked into the instrument, such that no proteins or detergents from previous tests would interfere with the measurements. The desorb routine involved rinsing the microfluidic system with 0.5% (w/v) sodium dodecyl sulfate and 50 mM glycine (pH = 9.5). Avidins were also manually spotted onto P3HT-modified gold substrates or printed onto the P3HT substrates using an automated dispensing platform (Biodot Prosys 5510A with a Biojet dispensing head equipped with a ceramic tip).

In flow immobilization, 300 μL of the avidin solution at a concentration of 50 μg/mL in PBS was injected at a flow rate of 20 μL/min for 15 min. Because of the difference in buffer composition of the various avidin stock solutions, bulk refractive index changes caused a small stepwise response, even after 20−50 times dilution in running buffer. These could be seen in kinetic adsorption curves in some cases. The immobilized amount of avidin was deduced from the difference in signal (in RU) before injection and after 5 min washing with PBS, taking 1 RU as 1 pg/mm^2. After adsorption, either 1 mg/mL pTHMMAA polymer solution was injected and/or 0.05% Tween 20 in PBS to block the surface against nonspecific adsorption. The biotinylated antibodies were allowed to attach to the avidins under similar conditions as the avidins by 15 min incubation from a 50 μg/mL solution in PBS. In some experiments, the antibody was also titrated in the concentration range of 70 ng/mL to 50 μg/mL.

Immobilization of avidin by manual pipetting was performed with the same concentration of avidin (50 μg/mL), dispensing 20−50 μL of solution onto the center of a P3HT chip, and allowing adsorption to occur for 20 min. The chip was then rinsed by pipetting and aspirating three portions of PBS, and thereafter 1 mg/mL pTHMMAA1 solution was dispensed onto the same area. Finally, the polymer was washed away with fresh milli-Q grade water, and blown dry with nitrogen. The chips were then stored in a desiccator before use. Alternatively, the avidins were printed onto P3HT chips as lines, 2 mm long and 0.6 mm wide, on areas corresponding to two of the four flow channels of the Biacore 3000 microfluidic system. In this case the avidins were dissolved in 30% glycerol solution in PBS, which prevented drying of the chips during the 20 min incubation time. After printing, the avidin solution was aspirated with a Pasteur pipet connected to a vacuum pump, and the surface washed with PBS and blocked with pTHMMAA1 as in the manual pipetting procedure. In this way, two active and two reference channels could be obtained for the successive depositions and measurements of antibody and antigen.

2.5. Assessment of Antibody Activity with SPR. A concentration analysis method was used over a broad concentration range to enable assessment of specific and nonspecific binding of antigen (h-IgG or CRP) to the biotinylated antibodies. The binding was studied in PBS running buffer, and antigen standards were diluted in PBS containing 0.5 mg/mL BSA (unless differently specified). Typically, 3-fold dilutions were made in the concentration range 0.6 ng/mL-100 μg/mL. The flow rate was 20 μL/min and the association time 15 min. The antigen binding was followed by 10 min desorption, taking a sample point after 5 min washing with PBS. Before titration, a blank matrix (0.5 mg/mL BSA in PBS) was injected until a constant value was attained per injection, and the background value caused by BSA was subtracted from the responses of the standards of antigen. Experimental binding curves were constructed by plotting the cumulative binding level after each injection of standard, and the curves were fitted to a dual-site Sips isotherm (eq 1) as previously described.[26] The parameters of the specific binding step at lower concentration were determined by nonlinear curve-fitting, using OriginLab version 7.5 (OriginLab Corp, MA, USA). The fitting procedure yielded the affinity constant, K_{A1}, the capacity constant, Γ_1, and the binding exponent, n_1, which represent the strength of binding, the density of binding sites, and the cooperativity of binding respectively. In case of n being smaller than unity one generally refers to anticooperativity. In practice, however, anticooperativity cannot be easily separated from heterogeneity of binding sites, unless there are clearly distinguishable steps in the binding isotherm, that can be modeled with multiple binding sites. From these fitted parameters the assay sensitivity (S), and binding efficiency (η), were derived (eqs 2 and 3). The sensitivity is the limiting condition where $c \ll 1/K_{A1}$, and represents the slope of the concentration versus response curve. The binding efficiency denotes the amount of binding sites that are active on the surface, relative to the total amount of binding sites, using the equivalent molecular weight of the antigen (M_r^{Ag}) and the antibody (M_r^{Ab}), and $\Gamma_{Ag} = \Gamma_1$.

$$\Gamma(c) = \frac{\Gamma_1(K_{A1}c)^{n_1}}{1 + (K_{A1}c)^{n_1}} + \frac{\Gamma_2(K_{A2}c)^{n_2}}{1 + (K_{A2}c)^{n_2}}, \text{ where } K_{A1} \gg K_{A2} \quad (1)$$

$$S = \Gamma_I K_{A1}^{n_1} \quad (2)$$

$$\eta = \frac{\Gamma_{Ag}}{\Gamma_{Ab}} \frac{M_r^{Ab}}{M_r^{Ag}} \quad (3)$$

2.6. AFM Imaging. Atomic force microscopy was conducted on a Park Systems XE100 system (Suwon, South-Korea), using high-resolution ACTA-SS cantilevers with a radius of curvature smaller than 5 nm (AppNano Inc., Santa Clara, CA, USA). The resonant frequency in air was 342−343 kHz, and the imaging was mostly performed by using noncontact mode (NC-AFM), while intermittent (tapping) mode (TM-AFM) was used for comparison. Scanning in XY and Z-direction was done under closed loop, and open loop control, respectively. A scanning frequency in the region 0.25−1 Hz, mostly 0.5 Hz, was used throughout the imaging. All polythiophene layers used in the study were scanned with NC-AFM to estimate the surface roughness (R_q) and the layer thickness. The thickness of the polymer layers was determined from small scratches that were made in the film with a steel needle. Samples of avidins onto P3HT were prepared by manual dispensing as described in §2.2, with P3HT substrates of 8 × 12 mm size, glued with double sticking tape on an AFM sample disk. The avidins were allowed to adsorb for 20 min in a covered Petri dish. The blocking polymer employed in the AFM measurements was pTHMMAA4 in PBS solution (1 mg/mL). Shortly before imaging, the layers were rinsed with Milli-Q water and excess liquid was removed with a short burst of inert gas from an air-duster (AT-tuote, Sippo, Finland, containing 1,1,1,2-tetrafluoroethane). It was noticed that pTHMMAA4 significantly decreased the risk of dewetting of the avidins when imaged in air, such that deposited layers could be analyzed in a time window of 15−240 min after removal of water.

For visualization of biomolecules, the surface areas scanned were typically 250 × 250 or 500 × 500 nm. The obtained raw images were subjected to line flattening in the X and Y direction and incidental glitches were removed. The images were not further processed, i.e., no filtering or spike removal was applied, and glitches that were systematic (caused by stiction) were not compensated. In some cases, when the tracking was especially good, noise was slightly reduced by adding together the forward and the backward scan.

3. RESULTS AND DISCUSSION

3.1. General Properties of the Spin-Coated P3HT Layers. The spin-coated polythiophene layers were fully characterized in terms of thickness and refractive index by SPR, while the surface roughness and thickness was also determined by AFM. The cumulative results are presented in Table S1 of the Supporting Information. The contact angles of the polythiophenes in water revealed a decreasing trend with increasing extent of carboxylic acid substitution: The contact angles of P3HT and P3HT-COOH15 layers were very similar (respectively 106° to 102°), but for P3CPT a notably smaller value (66°) was encountered. Thus, P3HT and P3HT-COOH15 surfaces should be considered as hydrophobic and P3CPT surfaces as mildly hydrophilic.

The refractive index of the polythiophenes (1.64−1.76) was expectedly higher than that of proteins, and the deduced values were generally also slightly higher than the theoretical value, which was calculated from the molar volume and the molar refractivity by extrapolation to high molecular weight.[27] Even thin layers of P3HT caused a large offset in the SPR angle. Although the starting angle for a blank gold chip on the Biacore 3000 instrument is ± around 11000 RU, the starting level for making measurements in the presence of the P3HT layer was typically 24 000−38 000 RU depending on the type (and concentration) of P3HT used. However, the starting angle and angular shift generally remained in the lower half of the dynamic range of the instrument (90 000 RU), and linearity at high RU values was checked by using samples of diverse thickness. The thickness of the P3HT layer was 7 ± 1 and 8.0 ± 0.1 nm in the case of films spun from 1.25 mg/mL concentration as determined by AFM and SPR, respectively, and 25 ± 2 nm when spun from 2.5 mg/mL (determined only by AFM). SPR measurements and immobilization studies were predominantly made using the thinner 7 nm layers.

In the optical microscope images, a very low amount of particles was discerned at the P3HT surface, and pin holes were very seldom observed in the AFM images. With spin coating from chloroform, the surface roughness was lower for the thinner layers (0.43 ± 0.03 nm) than for the thicker layers (0.83 ± 0.08 nm), and low enough to visualize adsorbed biomolecules with AFM, similarly as demonstrated earlier with spin coated films of polystyrene.[28] The determination of film thickness and refractive index with SPR, using measurements in two optical media,[23] yielded good agreement with the AFM determination in case of P3HT and P3HT-COOH15, but varied quite significantly in case of P3CPT. Likely, the P3CPT layers were less uniform due to the use of a solvent that evaporated much more slowly. In a recent study, solvents generally much more volatile than DMF were used for spin coating of P3HT on silicon substrates (hexane, chloroform, ethyl acetate, and dichloromethoane).[29] In our case, the films were much thinner and uniform compared to this study.

3.2. Avidin Film Formation under Hydrodynamic Flow Conditions. On the P3HT surface with a thickness of about 7 nm, all the four selected avidin types adsorbed in a very different fashion (Figure 1A), with the common feature always being a two-phase response: a fast rise within a few seconds, followed by a slow rearrangement or second adsorption or desorption phase. The wt-Avd adsorbed very fast reaching a plateau value at 2500 ± 120 pg/mm^2 after a characteristic dip indicative of a transient rearrangement. This surface coverage is lower than that for wt-Avd adsorbed on gold (3600 ± 250 pg/mm^2).[30] Streptavidin showed a slow desorption after the steep rise in surface concentration. This effect of "overshooting" adsorption is characteristic of desorption due to strong spreading of the protein on the surface, which displaces biomolecules having arrived later at the surface.[31] The final surface concentration of streptavidin, after 10 min adsorption/desorption, was 2300 ± 300 pg/mm^2. This is slightly lower than the surface coverage obtained for streptavidin attached to an ethylene-glycol-biotin layer and a self-assembled layer with 10% biotin groups (260 and 3600 ± 300 pg/mm^2, respectively).[32,33]

The chimeric avidins adsorb in a highly contrasting way to wild type avidin and streptavidin: no overshooting effect is noticed, and a maximum surface coverage about twice of that of wt-Avd was obtained (4400 ± 250 pg/mm^2 for ChiAvd and 5150 ± 250 pg/mm^2 for ChiAvd-Cys). ChiAvd shows a longer adsorption phase, not yet reaching a maximum after 15 min, and it also desorbs more than ChiAvd-Cys. This is likely due to the possibility of the latter compound to form disulfide bonds between the avidin molecules, stabilizing the attached layer.

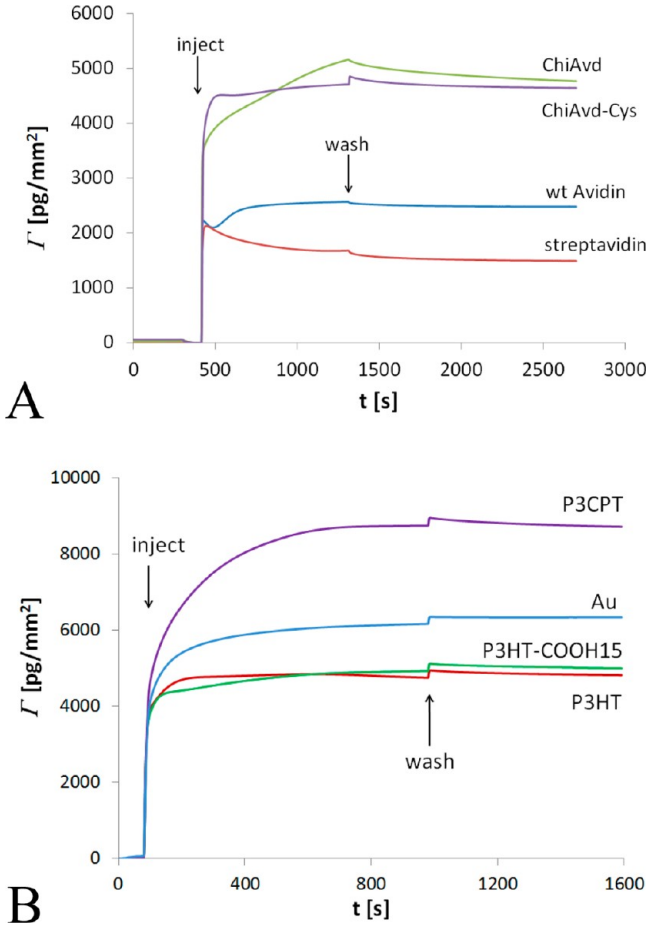

Figure 1. (A) Adsorption kinetics of four different avidins on P3HT at a concentration of 50 μg/mL in PBS at a flow rate of 20 μL/min, as measured on the Biacore 3000 instrument (n = 4). (B) Adsorption kinetics of ChiAvd-Cys on the three types of functionalized polythiophene, as compared to the adsorption on clean gold (n = 4). The ChiAvd-Cys concentration was 50 μg/mL in PBS and the flow rate 20 μL/min.

Avidin produced in *E. coli* with a molecular weight of about 59 kDa and a molecular size of 4.0 × 5.5 × 6.0 nm^3 would have a monolayer surface coverage of 3000 - 4450 pg/mm^2 depending on the orientation of the molecule[30] and these measures apply for chimeric avidin as well. Thus, monolayers with avidins standing on 4.0 × 5.5 nm^2 faces appear to have been formed for both ChiAvd and ChiAvd-Cys. The introduction of thiol groups increases the surface density of ChiAvd immobilized on P3HT similarly as is the case with thiolation of streptavidin immobilized on polystyrene, where introduction of thiol groups increased the biotin binding capacity even 3-fold.[34] It was proposed that thiolated streptavidin would give rise to a polymerized form of streptavidin, and the same condition can be proposed here for the ChiAvd-Cys (see further below).

Figure 1B depicts the kinetic results of ChiAvd-Cys adsorption to thin films of the three different polythiophenes used in this study. The gradual introduction of carboxylic acid groups amplifies the second adsorption phase, such that the final surface coverage of ChiAvd-Cys almost doubles for P3CPT compared with P3HT: after washing the surface, protein densities of 4800 pg/mm^2 are obtained for P3HT, 5000 pg/mm^2 for P3HT-COOH15, and 8800 pg/mm^2 for P3CPT. Compared to the adsorption onto gold (7000 pg/mm^2),[30] the P3CPT binds much more avidin, suggesting bilayer formation. This is likely due to the presence of long-range electrostatic interactions. This effect has been noticed also for polystyrene, and is the basis of the commercial "Maxisorp"-type polystyrene surface, in which the polystyrene has been made partly hydrophilic, having a contact angle of ±63°,[35] which is comparable to that of P3CPT. The adsorption of ChiAvd-Cys onto P3HT-COOH15 or P3HT is lower than that on gold, likely due to the strong hydrophobic adsorption, and spreading of the protein into a single monolayer.

3.3. Activity of Antibodies Immobilized under Flow Conditions. Since the antihuman IgG system has been much used in earlier work, it proved an appropriate reference system for preliminary evaluation of the effect of type of polythiophene and avidin on the binding constants, as measured with similar conditions and concentrations.[23] Under optimal conditions the affinity constant of the polyclonal anti-h-IgG Fab-fragment was of the order 2 × 10^9 M^{-1}. Thus, the binding parameters were determined for anti-h-IgG in its various forms and immobilized onto various avidins, and the results are summarized in Table 1. (The original binding curves are given in Figure S1 of the Supporting Information.)

First, the direct adsorption of various forms anti-h-IgG on the polythiophene surface was explored. Whole antibody, the F(ab′)$_2$-fragment and the biotinylated F(ab′)$_2$-fragment showed rather high affinity constants when attached directly to the surface (Table 1, entries 1−3, and Figure S1A of the Supporting Information), comparable to those measured earlier for F(ab′)$_2$ fragments immobilized/adsorbed directly onto gold. However, a low binding efficiency of about 5% or lower was observed. Especially the biotinylated F(ab′)$_2$-fragment gave a very low response upon passive adsorption. However, upon immobilization via various avidins the efficiency of binding rose to around 10%, which is much higher even than that of the nonbiotinylated antibodies physically adsorbed to P3HT (Table 1. Entries 4−8 and Figure S1.B of the Supporting Information). The ChiAvd-Cys, gave a nearly double capacity constant compared to the other avidins. In our results for P3HT it was thus found that the binding capacity of the antibody was greatly enhanced by the avidins, but the affinity constant was decreased compared to that measured for the physically adsorbed antibodies.

The overall influence of the introduction of 15% carboxyl groups in the polythiophene (with P3HT-COOH15) on the h-IgG binding was small (Table 1, entry 9), but for the fully carboxylated P3CPT the amount of ChiAvd-Cys and biotinyl-anti-h-IgG was noticeably higher (Table 1, entry 10). In the latter case, however, the amount of antigen bound was lower. It has been shown that the attachment of an antibody via biotin−avidin interaction may in some cases lead to a diminished binding affinity.[36] In our situation, it may be postulated that the loss of affinity is due to the strong increase in the surface concentration of the biotinylated probe causing steric interaction between the antigen molecules. When the values in Table 1 of K_A and Γ_{Ag} are plotted against each other, a roughly hyperbolic correlation could be observed when not considering the outlying value of the biotinyl-anti-h-IgG physically adsorbed to P3HT (see Figure S1C in the Supporting Information).

The generally low affinity of the polyclonal anti-h-IgG prompted a change to an analyte with more relevance to clinical diagnostic practice for which a biotinylated monoclonal antibody was available. As C-reactive protein (CRP) is an

Table 1. Overview of the binding characteristics of various Anti-h-IgG Antibodies Adsorbed on P3HT, P3HT-COOH, and P3CPT in the Presence and Absence of Avidin (n = 4)[a]

	type of									
no.	poly thiophene	avidin	antibody	Γ_{Avd} (pg/mm)	Γ_{Ab} (pg/mm^2)	Γ_{Ag} (pg/mm^2)	K_A ($\times 10^9$ M^{-1})	n	S ($\times 10^{14}$ pg/(mm^2 M))	η(%)
1	P3HT	none	whole antibody		2700 ± 160	360	1.26	1.29	2.0	
2	P3HT	none	F(ab′)$_2$		2400 ± 225	250	2.70	1.40	40	3.6
3	P3HT	none	biotinyl-F(ab′)$_2$		1450 ± 70	12	1.40	1.16	0.0048	0.3
4	P3HT	wt-Avd	biotinyl-F(ab′)$_2$	2500 ± 115	950 ± 50	350	0.27	0.88	0.0001	12.6
5	P3HT	b-Avd	biotinyl-F(ab′)$_2$	2950 ± 160	1200 ± 80	350	0.36	0.99	0.001	10.0
6	P3HT	Streptavidin	biotinyl-F(ab′)$_2$	2100 ± 330	1150 ± 180	300	0.69	1.13	0.031	8.9
7	P3HT	ChiAvd	biotinyl-F(ab′)$_2$	4400 ± 200	1150 ± 80	380	0.23	0.90	0.00014	11.3
8	P3HT	ChiAvd-Cys	biotinyl-F(ab′)$_2$	5170 ± 140	2000 ± 130	610	0.28	1.02	0.0027	10.4
9	P3HT-COOH15	ChiAvd-Cys	biotinyl-F(ab′)$_2$	5450 ± 150	2060 ± 90	620	0.19	1.00	0.0012	10.3
10	P3CPT	ChiAvd-Cys	biotinyl-F(ab′)$_2$	7260 ± 570	2820 ± 25	560	0.24	0.96	0.0006	6.8

[a]Antibodies and avidins were adsorbed in PBS buffer at 50 μg/mL, and both washed once with Tween 20 in PBS. Activity was measured in PBS buffer containing 0.5 mg/mL BSA, with h-IgG in the concentration range 0.0006−100 μg/mL (0.004−685 nM). Binding constants were evaluated according to eq 1, extracting the specific (high affinity) binding step. Γ_{Avd} = amount of avidin immobilized; Γ_{Ab} = amount of antibody (remaining after the Tween 20 washing step); Γ_{Ag} = capacity constant (maximum specific binding level of the antigen), K_A = Affinity constant, n = binding exponent; S = detection sensitivity (from eq 2); η = binding efficiency (from eq 3).

important general marker of infection and also recently used as a cardiac marker, a biotinylated, monoclonal anti-CRP was selected for subsequent experiments. As a first important issue, the effect of four avidins on the binding behavior of biotinylated anti-CRP to the avidins was screened, as well as the effect on the subsequent binding step of CRP (Figure 2). These experiments were performed on a single chip by injecting four different avidins in the four different channels of the Biacore 3000 system, after which all channels were used in titrations with anti-CRP and CRP. The different avidins interacted with the biotinylated anti-CRP at a very similar dissociation constant (40 nM) but there were notable differences in the end points and in the slopes of the titration curves: wt-Avd and streptavidin gave the most shallow binding curves with a slope less than expected for normal Langmuir binding (n = 0.8), whereas the curve of ChiAvd and ChiAvd-Cys were more steep than the Langmuir model (n = 1.3 and 1.7, respectively).

When evaluating the binding constants from the interaction of CRP to the anti-CRP (Figure.3.B), a significant improvement of binding was found for the chimeric avidins. Although the dissociation constant (K_D) was constant at around 15 nM (K_A = 0.67 × 10^8 M^{-1}), the specific binding capacity (Γ_{Ag}) varied strongly, and the highest value was found for ChiAvd-Cys (1100 ± 100 pg/mm^2).

Various types of pTHMMAA polymers have previously been employed as blocking agents for antibodies on gold surfaces or colloidal gold particles.[23,37] The amount of lipoate groups and type of linker was varied with the aim to arrive at an optimal performance of the antibody coating with respect to suppression of nonspecific binding and increase of stability of the antibody layer. In the present study, two polymers (pTHMMAA1 and pTHMMAA4) were selected for largely the same purposes, because of the consideration that these polymers contain a hydrophobic lipoate group attached to a hydrophilic polymer. Although the normal Tween 20 already worked reasonably well, the weakly amphiphilic nature of the pTHMMAA polymers was considered to render them quite serviceable as blocking agents on polythiophene surfaces, and they might possibly have some advantages over Tween 20. The pTHMMAA1 polymer contains 1 mol % of lipoate, whereas the pTHMMAA4 polymer contains 4 mol % lipoate. Therefore, intercalation based on hydrophobic interaction with P3HT was expected to be stronger for pTHMMAA4 than for pTHMMAA1. Indeed, flow injection experiments revealed that the pTHMMAA4 polymer gave a much higher surface coverage on P3HT (3400 ± 500 pg/mm^2) than pTHMMAA1 (800 ± 200 pg/mm^2). When adsorbing the pTHMMAA polymers from 1 mg/mL, the contact angle of P3HT decreased from 105 to 78° for pTHMMAA4 and 69° for pTHMMAA1.

The kinetic curves of binding of pTHMMAA1 to the P3HT surfaces modified with four different avidins evidenced that significant amounts of pTHMMAA1 were adsorbed in case of streptavidin and ChiAvd-Cys, but much less in case of wt-Avd and ChiAvd (for details, see Figure S2 of the Supporting Information). The effect of pTHMMAA1 addition on the binding of biotinylated anti-CRP to the avidins was determined in a similar way as performed in Figure 2 (see Figure S3A, B in the Supporting Information for the corresponding figures). The effect of the polymer on the binding of biotinylated anti-CRP to ChiAvd-Cys was not significant, but for streptavidin, 37% less anti-CRP was bound when the treatment with pTHMMAA1 was included. For ChiAvd and wt-Avd, the decrease in response was small (12−13%). The effect of treatment with pTHMMAA1 on the binding of CRP to the anti-CRP was largely parallel with the effects of binding of biotinylated anti-CRP to the avidins. Thus, blocking with the pTHMMAA1 can be applied in the case of ChiAvd-Cys, but cannot be advised for streptavidin. The results shown in Figure 1 suggest that streptavidin experiences significant unfolding and spreading on

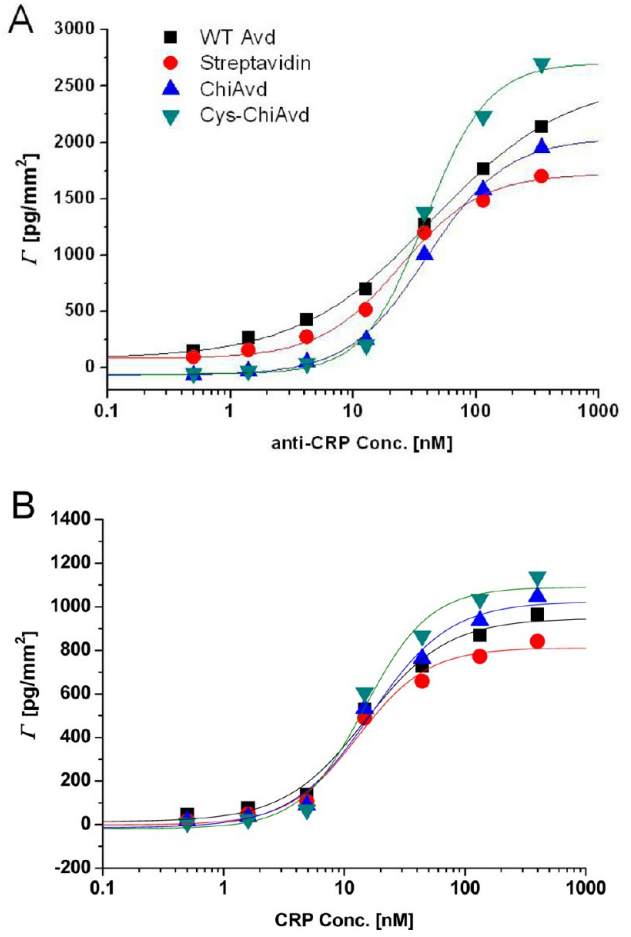

Figure 2. Simultaneous titration curves (symbols) with theoretical fit to the single-site Sips-isotherm (lines) of (A) the binding of biotinylated anti-CRP to four different avidins and (B) binding of the CRP to the anti-CRP. Measurements were performed by immobilizing the avidins in different channels, followed by injection in all channels of: (1) Tween 20 (0.05%) in PBS, (2) one blank injection of PBS, (3) increasing concentrations of biotinylated anti-CRP in PBS (0.07−50 mg/L in 3-fold dilutions), and (4) increasing concentrations of CRP in PBS (0.07−50 mg/L).

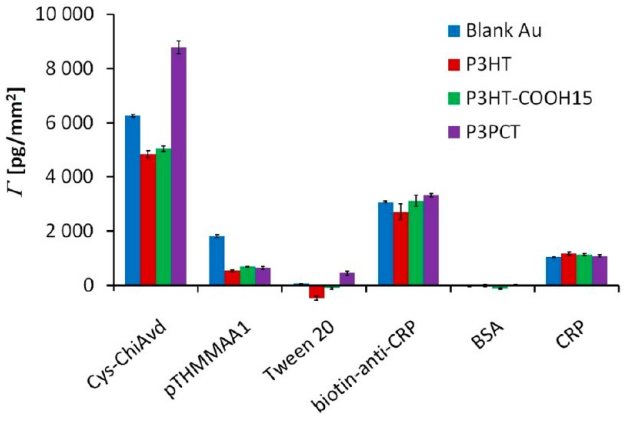

Figure 3. Immobilization levels of ChiAvd-Cys, biotinylated anti-CRP, and CRP on four different surfaces, together with the effects of blocking with pTHMMAA1, washing with Tween 20, and blocking with BSA (n = 4).

the surface, which is less apparent for other avidins. The more bulky pTHMMAA1 polymer may adsorb on top of the unfolded (inactivated) streptavidin molecules and thus impede the binding of the biotinylated probe to neighboring intact streptavidin molecules as well.

When comparing the effect of pTHMMAA1 and pTHMMAA4 on the on the binding of anti-CRP and CRP (with the ChiAvd-Cys-modified P3HT surface) the pTHMMAA1 gave better binding of both (see the Supporting Information, Figure S3C). There was a particularly large adsorption of Tween 20 after blocking with pTHMMAA1, whereas in the case of pTHMMAA4, there was a desorption effect with Tween 20, indicating weaker binding to the substrate. An efficient procedure was thus obtained for antibody immobilization, in which ChiAvd-Cys was first adsorbed from 50 μg/mL in PBS to the polythiophene surface, then blocked with pTHMMAA1 (1 mg/mL in PBS), and finally washed with Tween 20 (0.05% in PBS), thus employing two types of blocking agents sequentially. The biotinylated probe was then attached to the avidin (from 50 or 100 μg/mL in PBS) and the surface was blocked with BSA (0.5 mg/mL in PBS).

This more optimal immobilization scheme was finally tested with four different surfaces: P3HT, P3HT-COOH15 and P3PCT with blank gold as a reference, of which the results are summarized in Figure 3. First, it can be observed that the amount of pTHMMAA1 intercalating between the ChiAvd-Cys molecules is more than twice for the gold surface as it is for the polythiophene surfaces, but the Tween 20 washing effect is very minor, suggesting a rather stable attachment to the gold substrate. With the polythiophene surfaces, the effect of Tween 20 changes very strongly when increasing the amount of carboxyl groups: with P3HT some desorption is observed, whereas in the case of P3HT-COOH15 there is only very minor desorption. In contrast, the P3PCT-treated surface shows additional adsorption of Tween 20. This is likely related to the high amount of bound ChiAvd-Cys and its good stability, as observed in Figure 1A.

Generally, the differences in adsorption level of ChiAvd-Cys to the various surfaces are higher than the differences in binding of the biotinylated anti-CRP, while the binding of CRP varies even less. This suggests that under these conditions the maximum amount of CRP is reached that can be bound to the (2-dimensional) surface. As the amount of CRP bound is contrary to the trend in anti-CRP binding, this may indicate a crowding effect. The optimal ratio of CRP to anti-CRP was seen on the P3HT surface with a yield of binding sites (η) of 14%, which is slightly higher as in the case of anti-h-IgG (Table 1). Cross-reactivity was also measured of CRP to the antihuman IgG, and human IgG to anti-CRP (see Table S2 in the Supporting Information). This was 6% for CRP and 15.7% for human IgG.

3.4. Immobilization of ChiAvd-Cys by Manual and Automated Dispensing. For commercial application, it is of primary importance to be able to immobilize bioreagents by printing methods, such as inkjet printing, as it enables, for instance, the construction of immunochromatographic test strips, and protein arrays.[38] In the present work some initial assessment was made by printing the ChiAvd-Cys onto P3HT by using either a normal microliter pipet or a nanoliter dispensing instrument, as described above. The results of manual spotting with a pipet indicated that the ChiAvd-Cys can be printed without serious loss of activity, although the slope of the binding curve of CRP to anti-CRP slightly decreased compared to flow-immobilization (see Figure S4 in the Supporting Information). When the biotinylated probe is also

dx.doi.org/10.1021/am3008517 | ACS Appl. Mater. Interfaces 2012, 4, 4067−4077

printed, after printing the avidin first, and stored in dry form, a 50% loss of activity was observed toward CRP. In this case, an additional preservative, such as glucosamine, could still be added.[39]

With the Biodot inkjet printer it was possible to print small lines of ChiAvd-Cys onto a Biacore 3000 sensor chip modified with P3HT. With this approach the tiny drops dispensed (5 nL) dry rapidly, and as a remedy 30% glycerol was added to the dispensing solution. After incubation of the avidin, all channels were blocked with pTHMMAA1 solution (1 mg/mL). In this way, ChiAvd-Cys could be selectively patterned to selected channels of the fluidic system, and it was possible to observe biotinylated anti-CRP and CRP binding to the active areas, the nonactive areas working as a reference. Figure 4 presents the

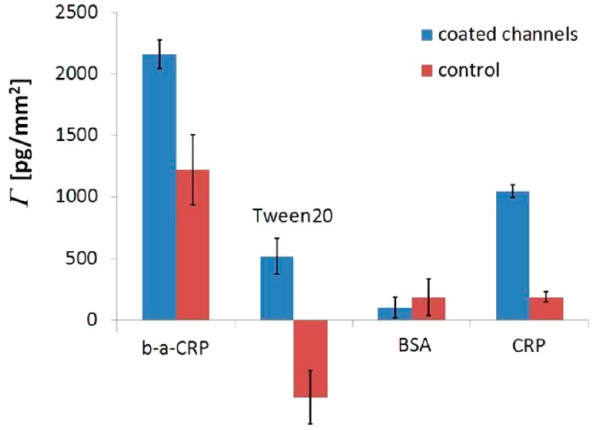

Figure 4. SPR response of ChiAvd-Cys immobilized by inkjet printing onto a P3HT substrate. Areas corresponding to two flow channels were spotted with ChiAvd-Cys, whereas two other areas corresponding to two other flow channels were left blank. All channels were then blocked with pTHMMAA1. SPR responses were measured to biotinylated anti-CRP ("b-a-CRP" one injection of 50 μg/mL), Tween 20 (0.05%, 2 injections, sum of two measurements shown), and BSA (500 μg/mL, sum of six injections shown), followed by titration with CRP up to 50 μg/mL (only final binding level shown in the bar plot).

SPR response to injections of biotinylated anti-CRP, Tween 20, BSA, and CRP. The results indicate a good discrimination between the blank and positive areas of the chip, with a relatively high washing effect for Tween 20 in the reference channels, which removes almost all adsorbed anti-CRP, whereas conversely in the avidin-modified channels, Tween 20 is adsorbed. The binding of CRP is comparable with that of the flow-immobilization method: a capacity constant of 700 $\pm$ 100 pg/mm^2 was found for CRP binding, an affinity constant of 1.1 $\pm$ 0.1 $\times$ 10^9 M^{-1} and a binding exponent of 1.0 $\pm$ 0.1 (n = 4). The binding efficiency was 15−18%, already 4 times better than the efficiency usually found with passively adsorbed antibodies (see Table 1). These results at least confirm that the ChiAvd-Cys is a highly effective scaffold for printing applications, as earlier demonstrated in another format.[12] The printing process, however, still has to be further optimized, because there was some nonspecific binding to the reference channels. The blocking polymer preferably should also be more firmly attached to the surface.

3.5. AFM Imaging of Avidins on P3HT. AFM imaging of the avidin molecules on the unmodified P3HT was performed in noncontact mode (NC-AFM) and tapping mode (TM-AFM). Results were obtained under comparable conditions, by allowing the avidins dissolved in PBS to adsorb onto the surface for 20 min, followed by washing with PBS and blocking with pTHMMAA4. The shorter pTHMMAA4 molecule was selected for AFM imaging because it gave avidin films that did not show dewetting upon drying in air. Imaging with NC-AFM generally gave the best resolution, as collected in Figure 5 for all the types of avidins, while other images with TM-AFM at different scales are collected in the Supporting Information. All types of polythiophene were routinely imaged with AFM after spin coating, but only P3HT was used for the imaging of the avidins. The P3HT polymer, when spin coated from 1.25 mg/mL chloroform, gave high-quality films with an average surface roughness of 0.43 $\pm$ 0.03 nm for NC-AFM (n = 12) and 0.35 $\pm$ 0.05 nm for TM-AFM (n = 5). On those surfaces no globular features could be discerned (Figure 5A). Neither PBS nor pTHMMAA4 increased the surface roughness significantly, but the pTHMMAA4 molecules could be indirectly observed in the phase contrast images in soft tapping mode on smaller areas, where a typical domain structure for polymers was visible (see Figure S5 in the Supporting Information).

Figure 5.B presents a P3HT surface treated with streptavidin (and blocked with pTHMMAA4), showing a rather uniform coating with slightly higher surface roughness (0.68 nm) when measured on the 500 nm image scale. Initially, there was a significant degree of stiction in the NC-AFM of the cantilever tip to the top features in the scanned area, which are seen as distinct depressions. The features of the molecular layer could be revealed more optimally with TM-AFM (see Figure S6 in the Supporting Information), particularly in the phase contrast image. Upon further drying, the features became shallow, and the stiction almost completely disappeared after a few hours.

In contrast to streptavidin, wt-Avd, when adsorbed to P3HT and blocked with pTHMMAA4, gave a rather uneven coating, with large pinholes (Figure 5C). Also in this case the tapping mode phase image revealed somewhat more detail (see Figure S-7B in the Supporting Information). Similarly as with streptavidin, stiction behavior in NC-mode was observed, which disappeared within a few hours. When using a smaller scan size and a faster sweep rate, more distinguishable globular features appeared with NC-AFM, and individual domains of about 12 nm in diameter became visible. This dimension is anticipated for wt-Avd in its folded conformation, taking into account the tip radius (see Figure S-7C,D in the Supporting Information).

In contrast to wt-Avd, the ChiAvd molecules adsorbed rather evenly and could be discerned as very small ellipsoids (Figure 5D). Because of the small size of the globular domains, scans were made on smaller surface areas in both imaging modes (see the Supporting Information, Figure S8). From these images, a typical size of the elliptic domains of approximately 9 $\times$ 13 nm^2 was measured, which would mean a domain size of 6 $\times$ 10 nm^2 when taking into account the tip dimension of 3−4 nm. In Figure 5E, an image of a P3HT surface is presented onto which ChiAvd-Cys molecules were adsorbed. These molecules adsorbed randomly in much larger clusters, with a specific height of about 4 nm, which is twice the height of the features observed for ChiAvd. The basic unit is here probably an oligomer of 3−5 units, which cluster further together in fibrils or small rings, which can be discerned at various locations in Figure 5E. With respect to the size of the ChiAvd monomer (4.0 $\times$ 5.5 $\times$ 6.0 nm^3), the height features are thus only about half of the theoretical height, which can be explained by various

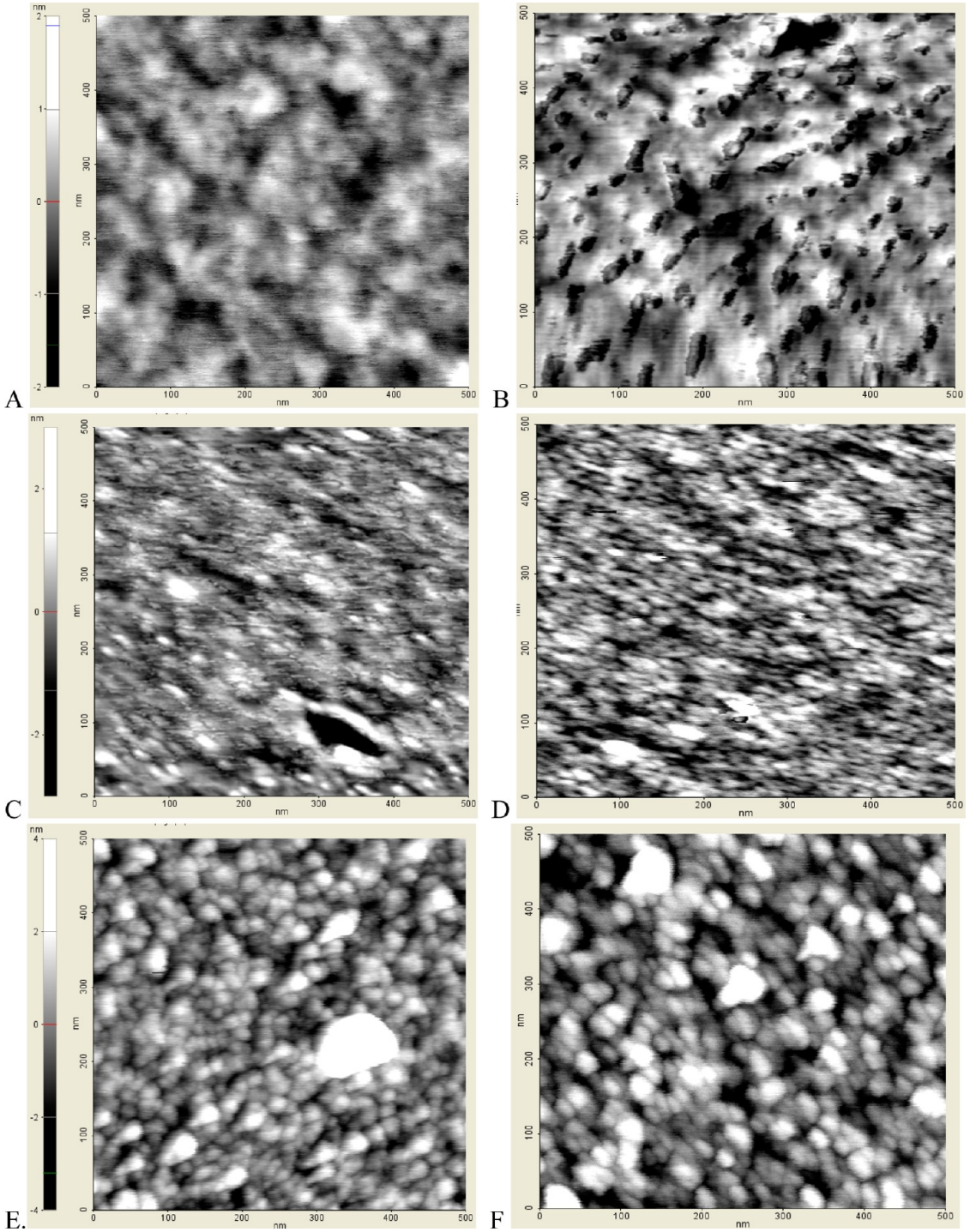

Figure 5. NC-AFM images (on 500 × 500 nm areas) of (A) blank P3HT and (B–E) avidins adsorbed to P3HT and blocked with pTHMMAA1: (B) Streptavidin; (C) wt-Avd; (D) ChiAvd; (E) ChiAvd-Cys; and (F) ChiAvd-Cys additionally treated with biotinylated anti-h-IgG F(ab′)$_2$.

conditions: (1) intrinsic factors of the AFM method,[40] (2) the filling-effect of the blocking polymer pTHMMAA4, and (3) a drying/flattening effect over time. The attachment of biotinyl-anti-h-IgG to the ChiAvd-Cys layer is observed also clearly in NC-AFM images (Figure 5F): even larger ellipsoids can be distinguished, which tend to coagulate similarly into small groups or rings. The characteristic feature height was here more variable (3–8 nm). In some cases dimers can be vaguely distinguished, which are likely dimers of F(ab′)$_2$-fragments rather than the subunits of single F(ab′)$_2$-fragments. The dimers were less resolved with TM-AFM, which pleads for the higher resolution and the less destructive nature of NC-AFM.

P3HT surfaces that had been coated with ChiAvd-Cys, biotinylated anti-CRP and CRP by the flow injection method in the Biacore 3000 instrument were also imaged with NC-AFM (Figure 6). In this case, much larger globular domains could be observed compared to those of Figure 5F: the feature heights ranged from 10 to 20 nm (Figure 6A). After CRP binding, the whole structure was rather sponge-like and rather resilient to flattening by drying. This points to a typical cross-linked

dx.doi.org/10.1021/am3008517 | ACS Appl. Mater. Interfaces 2012, 4, 4067–4077

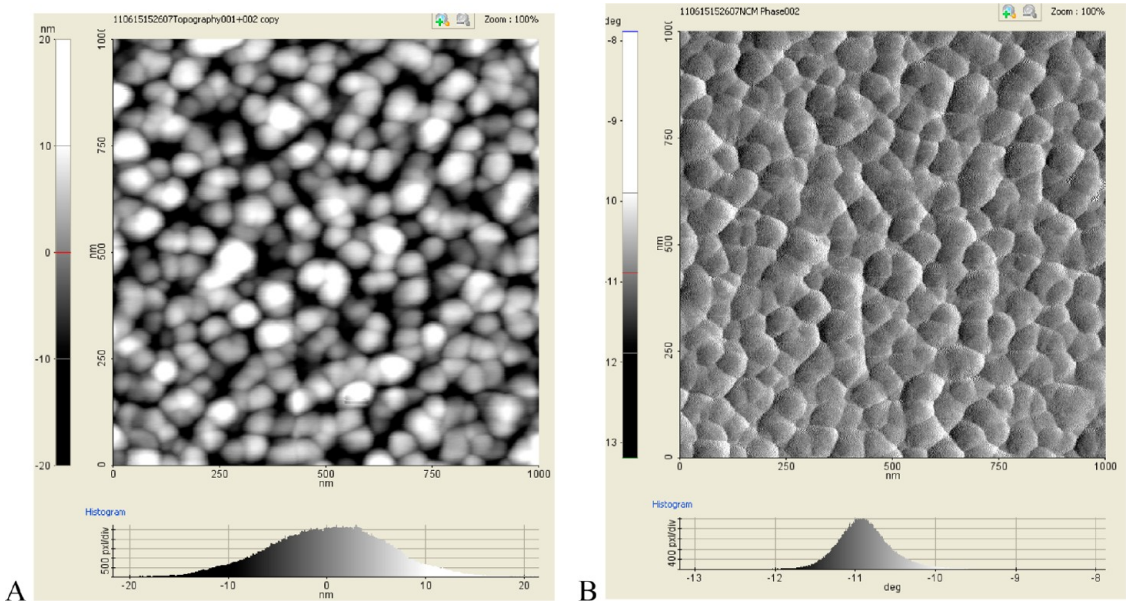

Figure 6. NC-AFM images (1 × 1 μm scale) of spotted ChiAvd-Cys, with bound anti-CRP, pTHMMAA4, BSA, and CRP. (A) topography, (B) phase.

immuno-complex formed from the reaction of CRP, a multivalent antigen, with the antibody. However, the subdomain structure of CRP, in the form of a pentamer, could not be visualized in NC-AFM.

4. CONCLUSIONS

The results support the view that the layer formation and stability of the chimeric avidin (ChiAvd), and particularly the cysteine-modified form (ChiAvd-Cys), on the different surfaces is significantly improved compared to wt-Avd and streptavidin. Not only the surface coverage of ChiAvd-Cys is higher, but it is also more resilient to desorption, induced by the blocking polymer pTHMMAA1 or Tween 20. The AFM images give evidence of a polymeric form of avidin, which likely stabilizes the deposition, and gives rise to a surface coverage almost equal to that calculated for a bilayer. The presence of a thiol-cross-linked polymeric form of ChiAvd-Cys is further evidenced by the observation that tris-carboxyethyl phosphine (TCEP), a disulfide splitting agent, causes strong dissociation/desorption of the ChiAvd-Cys from the P3HT surface already at a low concentration (1−5 mM), as measured with SPR. Furthermore, reduction by TCEP produces a monolayer of ChiAvd-Cys on gold.[30] The polymer formation of ChiAvd-Cys is thus similar as observed for thiolated streptavidin on polystyrene,[34] increasing the surface coverage of both avidin and the biotinylated antibodies.

With respect to the type of polythiophene used, a moderate increase in hydrophilicity and introduction of electrostatic interactions through carboxylic acid functions further increases the surface coverage of the ChiAvd-Cys, particularly for P3CPT. However, this does not give rise to an equally large increase of the binding of the biotinylated antibodies. The activity of biotinylated antibodies (to h-IgG and CRP) under hydrodynamic flow conditions could be optimized mainly with respect to the binding capacity, and the avidins in general gave higher yield of binding sites than obtainable by passive adsorption (10−14% level instead of 5%). With immobilization under hydrodynamic flow conditions, the binding levels for the ChiAvd-Cys varied greatly between the different surfaces, but the levels of anti-CRP and CRP binding were rather similar, with an optimum for the P3HT surface in the final binding reaction with CRP. Especially the ratio of bound antigen to antibody was much improved: the final yield of binding sites for the anti-CRP was 14%. Thus, it could be clearly observed that the ChiAvd-Cys allows immobilization of biotinylated probes to a wide variety of surfaces, yielding a consistent antigen binding. However, on the rather flat polythiophene surfaces there is a trade-off between the capacity and affinity, such that not necessarily the highest density of binding sites yields the greatest sensitivity at low antigen concentrations. A tentative optimum was found for P3HT. The ChiAvd-Cys molecule was also rather ideal for spotting and inkjet printing: preliminary results indicate that a 15−18% yield of binding sites is attainable and sufficiently high affinity and capacity constants for biotinylated antibodies attached to the printed chimeric avidin.

■ ASSOCIATED CONTENT

Ⓢ Supporting Information

Properties of the polythiophene films, reactivity and cross-reactivity of the anti-h-IgG and anti-CRP antibodies, activity of anti-h-IgG attached to P3HT surfaces, binding kinetics of avidins, titration curves of anti-CRP, and TM-mode AFM images. This material is available free of charge via the Internet at http://pubs.acs.org.

■ AUTHOR INFORMATION

Corresponding Author

*Tel: +358 40 5711328. Fax: +358 20 722 3498. E-mail: martin.albers@vtt.fi.

Notes

The authors declare no competing financial interest.

■ ACKNOWLEDGMENTS

Financial support from VTT, the Technical Research Centre of Finland, and from the European Union is gratefully acknowledged (EU-FP7 project BioEGOFET, Contract 248728). We

also thank Academy of Finland and Pirkanmaa Hospital District for financial support.

REFERENCES

(1) Butler, J. E.; Ni, L.; Nessler, R.; Joshi, K. S.; Suter, M.; Rosenberg, B.; Chang, J.; Brown, L.; Cantarero, A. *J. Immunol. Methods* **1992**, *150*, 77−90.
(2) Vikholm, I. M.; Albers, W. M. *Langmuir* **1998**, *14*, 3865−3872.
(3) Cantarero, L. A.; Butler, J. E.; Osborne, J. W. *Anal. Biochem.* **1980**, *105*, 375−382.
(4) Luppa, P. B.; Sokoll, L. J.; Chan, D. W. *Clin. Chim. Acta* **2011**, *314*, 1−26.
(5) Choulis, S. A.; Kim, Y.; Nelson, J.; Bradley, D. D. C.; Giles, M.; Shkunov, M.; McCulloch, I. *Appl. Phys. Lett.* **2004**, *85*, 3890−3892.
(6) Zen, A.; Pflaum, J.; Hirschmann, S.; Zhuang, W.; Jaiser, F.; Asawapirom, U.; Rabe, J. P.; Scherf, U.; Neher, D. *Adv. Funct. Mater.* **2004**, *14*, 757−764.
(7) Kanungo, M.; Srivastava, D. N.; Kumar, A.; Contractor, A. Q. *Chem. Commun. (Cambridge, UK)* **2002**, *2002*, 680−681.
(8) Lautner, G.; Kaev, J.; Reut, J.; Öpic, A.; Rappich, J.; Syritski, V.; Gyurcsányi, E. *Adv. Funct. Mater.* **2011**, *21*, 591−597.
(9) Nair, P. R.; Alam, M. A. *Nano Lett.* **2008**, *8*, 1281−1285.
(10) Katz, H. E.; Dodabalapur, A.; Bao, Z. Oligo- and polythiophene field effect transistors. In *Handbook of Oligo and Polythiophenes*; Fichou, D., Ed.; Wiley-VCH: Weinheim, Germany, 1999, Chapter 9.
(11) Laitinen, O. H.; Nordlund, H. R.; Hytonen, V. P.; Kulomaa, M. S. *Trends Biotechnol.* **2007**, *25*, 269−277.
(12) Heikkinen, J. J.; Kivimaki, L.; Määttä, J. A. E.; Makelä, I.; Hakalahti, L.; Takkinen, K.; Kulomaa, M. S.; Hytönen, V. P.; Hormi, O. E.O. *Colloids Surf., B* **2011**, *87*, 409−414.
(13) Laschewsky, A.; Rekai, E. D.; Wischerhoff, E. *Macromol. Chem. Phys.* **2001**, *202*, 276−286.
(14) Vikholm-Lundin, I. M. *Langmuir* **2005**, *21*, 6473−6477.
(15) Albers, W. M.; Auer, S. A.; Helle, H.; Munter, T.; Vikholm-Lundin, I. M. *Colloids Surf., B* **2008**, *68*, 193−199.
(16) Albers, W. M.; Munter, T.; Laaksonen, P.; Vikholm-Lundin, I. M. *J. Colloid Interface Sci.* **2010**, *348*, 1−8.
(17) Albers, W. M. *Sensor Element and Its Use*. Patent FI-120698 2010.
(18) Ferraris, J. P.; Yassar, A.; Loveday, D. C.; Hmyene, M. *Opt. Mater.* **1998**, *9*, 34−42.
(19) Suspène, C.; Miozzo, L.; Choi, J.; Gironda, R.; Geffroy, B.; Tondelier, D.; Bonnassieux, Y.; Horowitz, G.; Yassar., A. *J. Mater. Chem.* **2012**, accepted.
(20) Hytönen, V. P.; Määttä, J. A.; Nyholm, T. K.; Livnah, O.; Eisenberg-Domovich, Y.; Hyre, D.; Nordlund, H. R.; Hörhä, J.; Niskanen, E. A.; Paldanius, T.; Kulomaa, T.; Porkka, E. J.; Stayton, P. S.; Laitinen, O. H.; Kulomaa, M. S. *J. Biol. Chem.* **2005**, *280*, 10228−10233.
(21) Hytönen, V. P.; Laitinen, O. H.; Airenne, T. T.; Kidron, H.; Meltola, H, N. J.; Porkka, E. J.; Hörhä, J.; Paldanius, T.; Määttä, J. A.; Nordlund, H. R.; Johnson, M. S.; Salminen, T. A.; Airenne, K. J.; Ylä-Herttuala, S.; Kulomaa, M. S. *Biochem. J.* **2004**, *84*, 385−390.
(22) Määttä, J. A.; Eisenberg-Domovich, Y.; Nordlund, H. R.; Hayouka, R.; Kulomaa, M. S.; Livnah, O.; Hytönen, V. P. *Biotechnol. Bioeng.* **2011**, *108*, 481−90.
(23) Albers, W. M.; Vikholm, I. M. Surface Plasmon Resonance on Nanoscale Organic Films. In *Nano-Bio-Sensing*; Carrara, S., Ed.; Springer Verlag: Heidelberg, Germany, 2011; Chapter 4 , pp 83−125.
(24) *Biacore 3000, Instrument Manual*; GE/Biacore AB: Uppsala, Sweden, 2011.
(25) Vörös, J. *Biophys. J.* **2004**, *87*, 553−561.
(26) Sips, R. J. *J. Chem. Phys.* **1948**, *16*, 490−495.
(27) *ACD/ChemSketch Reference Manual Version 12.0*; Advanced Chemistry Development Inc.: Toronto, ON, 2010; pp 177−183.
(28) Qian, W.; Yao, D.; Yu, F.; Xu, B.; Zhou, R.; Bao, X.; Lu, Z. *Clin. Chem.* **2000**, *46*, 1456−1463.
(29) Zen, A.; Pflaum, J.; Hirschmann, S.; Zhuang, W.; Jaiser, F.; Asawapirom, U.; Rabe, J. P.; Scherf, U.; Neher, D. *Adv. Funct. Mater.* **2004**, *14*, 757−761.
(30) Vikholm-Lundin, I. M.; Auer, S.; Paakkunainen, M.; Määttä, J.; Munter, T.; Leppiniemi, J.; Hytönen, V. P.; Tappura, K. *Sens. Actuators, B* **2012**, in press.
(31) Andrade, J. D. Principles of Protein Adsorption. In *Surface and Interfacial Aspects of Biomedical Polymers, Vol. 2: Protein Adsorption*; Andrade, J. D., Ed.; Plenum Press: New York, 1985; Chapter 1 , pp 57.
(32) Lee, B. S.; Chi, Y. S.; Lee, K.-B.; Kim, Y.-G.; Choi, I. S. *Biomacromolecules* **2007**, *8*, 3922−3929.
(33) Yang, N.; Su, X.; Tjong, V.; Knoll, W. *Biosens. Bioelectron.* **2007**, *22*, 2700−2706.
(34) Ylikotila, J.; Välimaa, L.; Takalo, H.; Pettersson, K. *Colloids Surf., B* **2009**, *70*, 271−277.
(35) Technical data on polystyrene, obtained from Nunc A/S, Roskilde, Denmark, 2001. http://www.nuncbrand.com/files/en-656.pdf.
(36) Vijayendran, R. A.; Leckband, D. E. *Anal. Chem.* **2001**, *73*, 471−480.
(37) Vikholm-Lundin, I. M.; Albers, W. M. *Biosens. Bioelectron.* **2006**, *21*, 1141−1148.
(38) Xu, J.; Lynch, M.; Nettikadan, S.; Mosher, C.; Vegasandra, S.; Henderson, E. *Sens. Actuators, B* **2006**, *113*, 1034−1041.
(39) Kallmeyer, G.; Winter, G.; Klessen, C.; Woog, H. PCT Patent No. WO9822136, 1998.
(40) Morris, V. J.; Kirby, A. R.; Gunning, A. P. Macromolecules. In *Atomic Force Microscopy for Biologists*; Imperial College Press:, London, 2010; Chapter 4 , pp 130−136.